Mapping coastal marine debris using aerial imagery and spatial analysis☆

Kirsten Moy[a,*], Brian Neilson[b], Anne Chung[a], Amber Meadows[a], Miguel Castrence[c],
Stephen Ambagis[c], Kristine Davidson[a]

[a] Social Science Research Institute, University of Hawaii at Manoa, 2424 Maile Way, #718, Honolulu, HI 96822, USA
[b] Division of Aquatic Resources, Department of Land and Natural Resources, 1151 Punchbowl St. #330, Honolulu, HI 96813, USA
[c] Resource Mapping Hawaii, PO Box 492230, Keaau, HI 96749, USA

ARTICLE INFO

ABSTRACT

This study is the first to systematically quantify, categorize, and map marine macro-debris across the main Hawaiian Islands (MHI), including remote areas (e.g., Niihau, Kahoolawe, and northern Molokai). Aerial surveys were conducted over each island to collect high resolution photos, which were processed into orthorectified imagery and visually analyzed in GIS. The technique provided precise measurements of the quantity, location, type, and size of macro-debris ($> 0.05 \text{ m}^2$), identifying 20,658 total debris items. Northeastern (windward) shorelines had the highest density of debris. Plastics, including nets, lines, buoys, floats, and foam, comprised 83% of the total count. In addition, the study located six vessels from the 2011 Tōhoku tsunami. These results created a baseline of the location, distribution, and composition of marine macro-debris across the MHI. Resource managers and communities may target high priority areas, particularly along remote coastlines where macro-debris counts were largely undocumented.

1. Introduction

Marine debris presents physical, biological, and chemical threats to coastal ecosystems (Coe and Rogers, 1997; Derraik, 2002; Sheavly and Register, 2007; EPA, 2011; Gall and Thompson, 2015). It can degrade habitats through smothering, abrasion, and fragmentation, ultimately leading to mortality of benthic species, particularly corals (Donohue et al., 2001; Asoh et al., 2004; Chiappone et al., 2005). Large marine debris is known to transport nonnative biofouling species (Ghaderi and Henderson, 2013; Calder et al., 2014; Carlton, 2015). Furthermore, it can negatively affect marine wildlife through entanglement, which can harm fish (Romeo et al., 2015; Cannon et al., 2016), birds (Wilcox et al., 2015), turtles (Nelms et al., 2016), marine mammals (Henderson, 2001; Derraik, 2002; Attademo et al., 2015), and invertebrates (Donohue et al., 2001; Asoh et al., 2004; Setälä et al., 2016). Chemical contaminants can be transported, leach into the environment, and transfer to wildlife (Rios et al., 2007; Teuten et al., 2009). All of these threats can compromise the balance of marine ecosystems, resulting in costly control efforts, cleanups, and negative economic impacts (Mouat et al., 2010).

Hawaii historically has the highest reported debris accumulations for United States' Pacific Ocean coastlines (Ribic et al., 2012a). This influx of marine debris is attributed to the state's proximity to the North Pacific Subtropical Gyre (Howell et al., 2012) and the Subtropical Convergence Zone (Ribic et al., 2012a). In addition, the 2011 Tōhoku tsunami swept millions of metric tons of large detritus into the ocean (Headquarters for Ocean Policy, 2013). This litter began arriving on U.S. shores in the winter of 2011–2012 and continued to arrive in Hawaii through 2016 (Carlton et al., 2017). Multiple pieces of Japanese tsunami marine debris (JTMD) were found to host non-native species, representing a potential vector of invasive introductions (Derraik, 2002; Choong and Calder, 2013; Gewin, 2013; Calder et al., 2014; Carlton et al., 2017). Thus, marine debris accumulation in Hawaii is a pressing threat, especially following a major natural disaster.

Our understanding of marine debris accumulation patterns and composition in Hawaii is limited both in scale and scope. Previous studies focused on Oahu (Ribic et al., 2012a), Hawaii Island (Carson et al., 2013), Maui (Blickley et al., 2016), Midway Atoll (Ribic et al., 2012b), and Kure and Pearl and Hermes Atolls (Dameron et al., 2007). Hawaii-based studies have also addressed specific debris types in the state, such as derelict fishing gear (Donohue et al., 2001; Boland and Donohue, 2003; PIFSC, 2010), and plastics (Corcoran et al., 2009; Cooper and Corcoran, 2010; Kwon et al., 2014; Young and Elliott, 2016). There has not been a comprehensive quantification of marine

debris in the main Hawaiian Islands (MHI) to date. The challenges of such an effort in the MHIs include the shorelines' ruggedness and inaccessibility, and the extensive distance that must be reconciled with time available and the level of detection and detail. A large-scale and systematic surveillance and spatial analysis technique is required to successfully map the entirety of the MHI.

This effort is the first study to use orthorectified aerial imagery to identify and categorize marine macro-debris in the MHI. The aim of this study was to (1) locate, quantify, and categorize debris, (2) map hot spots (areas of high debris accumulation), and (3) find and physically verify putative JTMD vessels. Creating a comprehensive baseline of marine macro-debris patterns across the entirety of the MHI assists both managers and community groups in prioritizing future debris removal efforts, particularly following major natural disasters in the Pacific Ocean.

2. Materials & methods

2.1. Aerial imagery collection and processing

To collect coastal imagery, aerial surveys were conducted over the coastlines of the main Hawaiian Islands of Niihau, Kauai, Oahu, Molokai, Lanai, Maui, Kahoolawe, and Hawaii (Fig. 1) using a Cessna 206. Sixteen missions were flown on fourteen separate days from August to October 2015 during optimal weather conditions to minimize cloud cover and avoid high winds and turbulence (Table 1). Areas where flight restrictions apply, such as military bases and airports, were excluded from the imagery collection process.

Photos were collected at a target overlap of 60% and an altitude of 610 m above ground level (AGL). This produced the final orthorectified imagery mosaics at 2 cm ground sample distance (GSD) and covered a swath of 300 m. The remote sensing system (Icaros IDM600) included two DSLR cameras (Canon EOS 5DS R) and one medium format aerial camera (Phase One P65 +) mounted on a three-axis gyro-stabilized gimbal to ensure that all photos were taken within 4 degrees of roll, pitch and yaw. Real-time, differentially corrected GPS data was obtained through the OmniSTAR satellite-based augmentation system. Raw camera data was converted and corrected for lens distortion, variable lighting, and systematic noise reduction or image sharpening using Capture One Pro (Phase One, 2015).

The aerial photos were synchronized with corresponding data on latitude, longitude, altitude, roll, pitch, and yaw. A standard photogrammetric aerial triangulation routine was performed in Icaros Photogrammetry Suite (Icaros, Inc., 2014). Each block of data was then

Fig. 1. Site map of the main Hawaiian Islands (MHI) showing the survey area (main) and location with respect to the North Pacific Subtropical Gyre (inset).

Table 1
Aerial survey dates. Flight time estimates are based on shoreline length and target ground speed. Total number of hours was 38.9, which includes time spent in transit from airports, delays, missed attempts due to weather conditions and air traffic, and extra passes required over complex shorelines.

Island	Shoreline (mi)	Dates surveyed	Estimated flight times (h)
Hawaii	392	Aug 7–9; Sept 1	4.1
Maui	192	Sept 7	2
Oahu	237	Sept 24	2.4
Molokai	119	Sept 23–24	1.2
Kauai	125	Oct 5–7	1.3
Lanai	58	Sept 9	0.6
Niihau	52	Oct 6	0.5
Kahoolawe	43	Sept 8	0.4

processed to obtain a within-model root-mean-square error (RMSE) of 1.5 m. Since only data from the aircraft's positions in the air was used without any ground control points, horizontal position errors ranged between 8 and 10 m. Finally, the imagery was color balanced and dodged to create a seamless mosaic and exported into uncompressed GeoTIFF tiles in the NAD 1983 UTM Zones 4N and 5N reference systems to correspond with existing GIS data layers. To ensure systematic analysis coverage, the imagery tiles were divided into numbered 1.6 km segments of coastline, which were overlaid onto the mosaics as a line shapefile in ArcGIS (ESRI, 2011). Out of the 1223 segments, imagery for 122 segments (10%) was not analyzed due to blurring or gaps resulting from airspace restrictions.

2.2. Marine debris analysis

Prior to detailed examination of the data, all analysts calibrated their efforts by processing the same set of imagery spanning approximately 76 km of coastline and comparing results. Data discrepancies were discussed among them to improve consistency and protocols were updated accordingly. In addition, randomly selected segments representing 20% of each island's coastline were re-analyzed to assess consistency among analysts and calculate a survey error associated with macro-debris detections.

The team visually panned through the imagery tiles and assigned every discernable debris item with a unique identification number. ArcGIS software (ESRI, 2011) was used to determine the latitude and longitude of each item. Eight categorical classifications (Table 2) were developed based on categories in Lippiatt et al. (2013) and the Alaska Department of Environmental Conservation tsunami debris aerial surveys (DEC, 2015). Analysts then recorded the macro-debris category by using photographic examples and visual characteristics such as shape and color for comparison (Fig. 2). Features, such as straight edges, spherical or conspicuous shape, and bright colors, assisted in the identification and classification of debris items. Items that could not be clearly identified in any of the eight categories were classified as "inconclusive." Those items that could be identified, but did not fit into the pre-determined categories, were classified as "other."

In addition, the ArcGIS measuring tool was used to determine the visible surface area of macro-debris items. Area measurements were grouped into four size classes: very small ($< 0.5\ m^2$), small ($0.5–1.0\ m^2$), medium ($1.0–2.0\ m^2$), and large ($> 2.0\ m^2$). Image resolution allowed for visual recognition of items as small as approximately $0.05\ m^2$. However, if a smaller debris item could be confidently detected, it was recorded. The 1.6 km segments were then categorized by debris density. To create the hotspots maps, the segments were regrouped into 8 km lengths to improve visual usefulness at a statewide scale, and any individual 8 km segment containing 100 debris items or more was considered a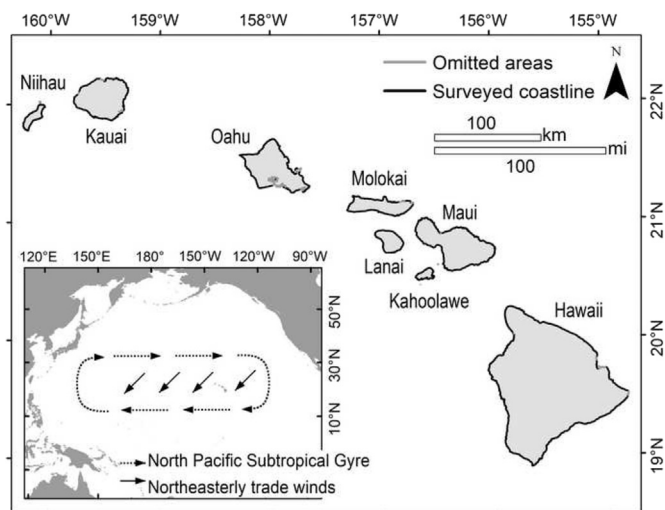 hotspot of debris accumulation.